Spacecraft Alignment Determination and Control for Dual Spacecraft Precision Formation Flying

Philip C. Calhoun[1] Anne-Marie Novo-Gradac[3], and Neerav Shah[2]
NASA Goddard Space Flight Center, Greenbelt, MD, 20771

Many proposed formation flying missions seek to advance the state of the art in spacecraft science imaging by utilizing dual-spacecraft precision formation flying (PFF) to enable a "virtual" space telescope. Using precision dual-spacecraft alignment, very long focal lengths can be achieved by locating the optics on one spacecraft and the detector on the other. Proposed science missions include astrophysics concepts with spacecraft separations from 1000 km to 25,000 km, such as the Milli-Arc-Second Structure Imager (MASSIM) and the New Worlds Observer, and heliophysics concepts for solar coronagraphs and X-ray imaging with smaller separations (50m – 500m). All of these proposed missions require advances in guidance, navigation, and control (GN&C) for PFF. In particular, very precise alignment control and estimation is required for inertial pointing of the virtual space telescope to enable science imaging orders of magnitude better than can be achieved with conventional single spacecraft instruments. For many applications, the PFF dynamics is coupled through the GN&C system when utilizing relative ranging and position alignment sensor components not co-located with the respective spacecraft mass centers. This work develops design architectures, algorithms, and performance analysis of GN&C systems for precision dual spacecraft inertial alignment. These systems employ a variety of GN&C sensors and actuators, including laser-based alignment and ranging systems, optical imaging sensors (e.g. guide star telescope), inertial measurement units (IMU), as well as microthruster and precision stabilized platforms. A comprehensive GN&C performance analysis is given for a heliophysics dual-spacecraft PFF imaging mission concept.

Nomenclature

$\bar{b}_{\omega_F}$	=	Gyro Measurement Bias for Follower Spacecraft
$\bar{b}_A$	=	Accelerometer Measurement Bias
m_F	=	Follower Spacecraft mass
q	=	Attitude Quaternion
$\bar{r}_{iF}$	=	Follower Spacecraft Position relative to i^{th} Central Body
$\bar{r}_A$	=	Accelerometer Location Vector relative to c.g.
$\bar{r}_E$	=	Environmental Disturbance Action Point Location Vector relative to c.g.
$\bar{r}_T$	=	Thruster Location Vector relative to c.g.
$\bar{u}_{F_E}$	=	Environmental Disturbance Specific Force on Follower Spacecraft
$\bar{u}_{F_{T_0}}$	=	Nominal Thruster Specific Forces for Control of Follower Spacecraft
$\bar{u}_R$	=	Leader/Follower Total Differential Specific Force
$\bar{u}_{thrust,F}$	=	Thruster Specific Force on Follower Spacecraft
$\bar{u}_{thrust,L}$	=	Thruster Specific Force on Leader Spacecraft

[1] Senior Aerospace Engineer, Attitude Control System Engineering Branch, MS 591, 8800 Greenbelt Rd. Greenbelt, Md. 20771,
[2] Associate Branch Head, Navigation and Orbit Design Branch, MS 595, 8800 Greenbelt Rd. Greenbelt, Md. 20771.
[3] Senior Aerospace Engineer, Heliophysics Branch, MS 672, 8800 Greenbelt Rd., Greenbelt, Md. 20771.

$\bar{x}$	=	Relative Spacecraft Position
I_F	=	Follower Spacecraft Inertia
$\bar{R}^{ref}$	=	Nominal Relative Spacecraft Position
$\ddot{\bar{\delta}}_F^m$	=	Follower Spacecraft Measured Acceleration
$\bar{\delta}_R$	=	Perturbed Relative Spacecraft Position
$\bar{v}_{\omega_F}$	=	Gyro Measurement Noise for Follower Spacecraft
$\bar{v}_A$	=	Accelerometer Measurement Noise
μ_i	=	Gravitational Constant for i^{th} Central Body
$\bar{\theta}$	=	Attitude Vector
θ_L	=	Leader Spacecraft to Astrometric Sensor boresight alignment angles
θ_G	=	Guide Star to Astrometric Sensor boresight alignment angles
θ_{δ_R}	=	Relative Spacecraft Alignment Angles
$\bar{\omega}$	=	Angular Rate Vector
$\Delta \bar{f}_{solar}$	=	Leader/Follower Differential Solar Pressure Specific Force
$\Delta \bar{f}_{pert}$	=	Leader/Follower Differential Gravitational Perturbations
Γ_{GG}	=	Gravity Gradient Perturbation to Relative Spacecraft Alignment Dynamics

I. Introduction

MANY proposed formation flying missions seek to advance the state of the art in spacecraft science imaging by utilizing dual-spacecraft precision formation flying (PFF) to enable a "virtual" telescope. The virtual telescope (VT) is formed by inertial alignment of an Optics (or Occulter) spacecraft (S/C) relative to a Detector S/C at a nominally fixed separation, depending on the telescope focal length. A functioning telescope with very long focal lengths can be achieved in this manner using precision dual-spacecraft alignment. Proposed virtual telescope science missions include astrophysics investigations using formation flying spacecraft with separations from 1000 km to 25,000 km, such as the Milli-Arc-Second Structure Imager (MASSIM)[1] and the New Worlds Observer (NWO)[2], and heliophysics concepts for solar coronagraphs, and x-ray imaging[4] with smaller separations (50m – 500m)[3]. All of these proposed missions require advances in precision formation flying of two spacecraft. In particular, very precise inertial alignment control and estimation is required for inertial pointing of the "virtual" telescope to enable science imaging orders of magnitude better than can be achieved with conventional single spacecraft instruments. Figure 1 shows the dual-spacecraft inertial (e.g. astrometric) alignment concept for a Leader/Follower formation flying architecture in which a single optical sensor mounted on a Follower S/C for tracking the Leader S/C relative to an inertial guide star target within the same sensor field of view.
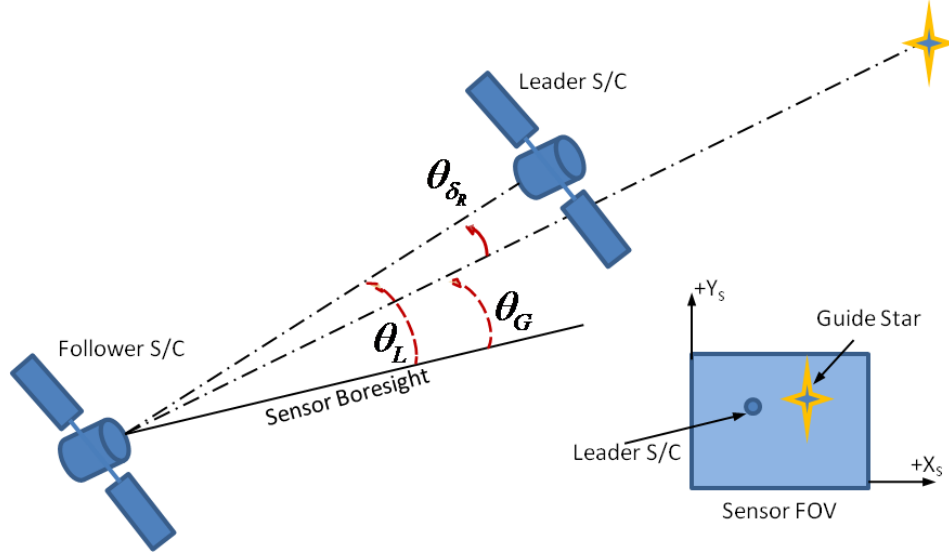
American Institute of Aeronautics and Astronautics

Figure 1. Dual-Spacecraft Precision Inertial Alignment Sensing Architecture.

This work develops the design of GN&C models and architectures necessary to implement onboard systems for dual-spacecraft PFF VT alignment. These systems employ a variety of GN&C sensors and actuators, including laser-based alignment and ranging systems, optical imaging sensors (e.g. guide star telescope), inertial measurement units (IMU), as well as microthruster and precision stabilized image motion compensation systems. Previous work included a consider-state analysis method for evaluation of dual-spacecraft relative navigation and architectures for precise inertial alignment[5]. That work focused on transverse alignment only because those degrees of freedom are the most critical for precision GN&C for the VT. In section II we extend the analysis to include all translational and rotational degrees of freedom for a more generic VT specification including attitude and range states. For many applications, the PFF dynamics are coupled through the GN&C system when utilizing relative ranging and position alignment sensor components not co-located with the respective spacecraft mass centers. A systematic method for relating the basic VT science instrument specifications for image smear and depth of focus to the attitude and translational requirements is developed in section II. This method is then used to develop models for the relative position and alignment measurements from optical sensors to be used in the GN&C framework for control design.

Section III includes a summary of a complete dynamics and control model framework for the development of alignment estimation and control algorithms. It includes a review of the basic equations for relative flight dynamics of two spacecraft flying in precise formation, based on previous studies by numerous authors[5]. In this paper, we use Luquette's formulation[6-9] of the relevant dynamics in an inertial reference as a basis for the GN&C design and analysis. The section also summarizes relevant inertial sensor compenent models, as developed by Calhoun[5]. The models developed in sections II and III form a framework for full state alignment filter and control system design methods. Section IV provides an example GN&C design application for PFF of a proposed Heliophysics VT mission concept.

II.   Virtual Telescope (VT) Stability Requirements and Measurement Models

It is difficult to develop deployable optical metering structures for large monolithic space telescopes (focal length > 50m) to achieve precise optics and detector alignment stability, within reasonable constraints on structural design for satellites. Precision formation flying of separate free-flying platforms for optics and detectors may be used to "replace" the optical metering structure, providing a stable platform for alignment of optics and detector. This establishes a "virtual" platform for telescope pointing and stability. This type of precision formation flight places unique requirements on the separated optics and detector platform dynamics and control, involving nine degrees of freedom (DoF) to fully characterize the image smear and stability of the depth of focus. The usual GN&C approach for a dual-spacecraft rendezvous, proximity operation, or constellation management, involves at most the relative six degrees of freedom between platforms since the inertial alignment of the two free flying vehicles it usually not relevant to formation flying. In this section, we develop the equations for the VT science imaging smear and depth of focus as a function of the nine DoF inherent in dual-spacecraft inertial alignment. This method is also applied to

the development of measurement models for optical alignment and ranging systems.

A. VT Attitude and Translation Stability Requirements

The first step in the GN&C design and analysis of the systems and architectures for VT formation flying is to derive requirements for the six attitude and three translational degrees of freedom for the dual-spacecraft formation as a function of the science imaging requirements at the detector. Figure 2 shows a breakdown of attitude and translational displacements starting from an ideal alignment of the detector and optics in a VT arrangement (shown in blue). The green frame represents translational displacement of optics off the line-of-sight from detector to target. The red frame represents rotational motion for both Optics S/C and Detector S/C. The resulting shift in optics center of focus from detector center is shown in Figure 2. From inspection of Fig. 2 it can be deduced that the image stability, $\vec{\delta}_I$, in terms of image smear, s_x, s_y, and depth of focus, d, is expressed in terms of the spacecraft relative translational $\vec{\delta}_R$, and absolute rotational, $\bar{\theta}_D$, $\bar{\theta}_O$ DoF as,

$$\vec{\delta}_I = \begin{bmatrix} s_x \\ s_y \\ d \end{bmatrix} = \left[\bar{P}_D + \bar{P}_{DO} + \vec{\delta}_R - \bar{P}_O + R(\bar{\theta}_O)\bar{P}_O + f(R(\bar{\theta}_O))\bar{P}_{OD} \right] - R(\bar{\theta}_D)\bar{P}_D. \tag{1}$$

Where the rotational operators, $R(\bar{\theta})$, can be expressed in terms of a small angles using cross product operator, $\tilde{\theta}$,

$$R(\bar{\theta}) = [I + \tilde{\theta}] . \tag{2}$$

The function, $f()$, is a mapping of focal plane image distortion (i.e. smear and depth of field) due to small rotations of the Optics platform, $R(\bar{\theta}_O)$. This effect on VT center of focus is illustrated in Fig. 2 by slight rotation of the optical imaging due to the Optics S/C rotation. This would in general be non-linear and dependent on the optics design, but could be linearized for small angles, as

$$f(R(\bar{\theta}_O)) = [I + {}^n\tilde{\theta}_O], \quad {}^n\bar{\theta}_O = \Phi\bar{\theta}_O, \quad \Phi \text{ is diag matrix, } 0 < \phi_i < 1 . \tag{3}$$

Where the scaling factors, ϕ_i, are derived from the optics design. These factors would be quite small for diffractive optics used for many x-Ray and UV optics in proposed VT applications. Combining (2) and (3) into (1) provides a simplified representation that serves as a basis for error analysis of image distortion in terms of requirements for the attitude and translation DoF.

$$\vec{\delta}_I = \begin{bmatrix} s_x \\ s_y \\ d \end{bmatrix} = \tilde{P}_D^x \bar{\theta}_D + \left[\Phi\tilde{P}_{DO}^x - \tilde{P}_O^x \right]\bar{\theta}_O + \vec{\delta}_R . \tag{4}$$

Equation 4 represents the coupling of the attitude and translational DoF for science imaging when the separated detector and optics components are not co-located with their respective spacecraft mass centers.
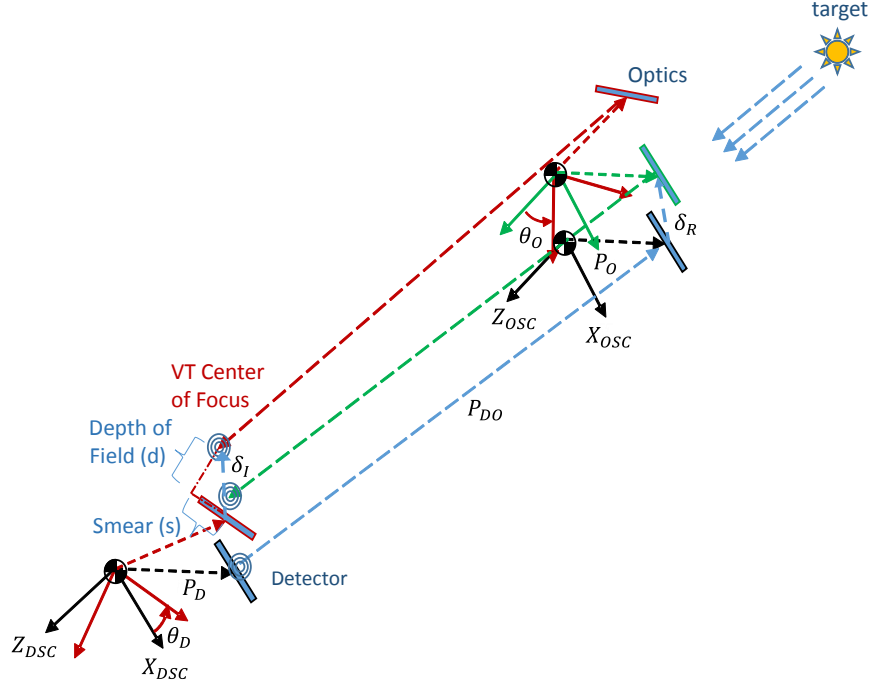
Figure 2**. Detector Image Smear and Depth of Focus as function of Attitude and Translation.**

B. VT Optical Alignment and Ranging System Measurement Models

The method used in Sec. A. to develop the science imaging requirements can also be used to model the relative position measurement for various optical (i.e. laser and camera) alignment and ranging components, illustrating this same 9 DoF coupling in the GN&C system design.

A laser alignment (a.k.a. laser metrology) system utilizes a detector mounted on the Detector S/C to measure the lateral alignment offset of an illuminated spot from a collimated laser source mounted on Optics S/C[10]. A non-collocated laser ranging system is also used to precisely measure the relative range. Then we can use Eq. (4) as a laser alignment and ranging measurement model by replacing appropriate variables,

$$\vec{\delta}_L = \begin{bmatrix} l_x \\ l_y \\ r_l \end{bmatrix} = \tilde{P}_L^x \, \vec{\theta}_D + \left[\Phi \, \tilde{P}_{LB}^x - \tilde{P}_B^x \right] \vec{\theta}_O + \vec{\delta}_R . \tag{5}$$

Where $\vec{\delta}_L$, represents the measured displacements from laser spot detector center, in terms of alignment (a.k.a. centration) errors, l_x , l_y, and ranging errors, r_l. The variables, $\tilde{P}_L^x , \tilde{P}_B^x , \tilde{P}_{LB}^x$, represent the cross product operators for position vectors of the laser detector elements on the Detector S/C, the laser beacon elements on Optics S/C, and the relative position from laser detectors to beacons, respectively. For this model, ϕ_i is set equal to 1 for a fixed-mounted laser beacon or set equal to 0 if beacon is collocated with the detector and a corner cube reflector, mounted on Optics S/C, servers as the virtual beacon.
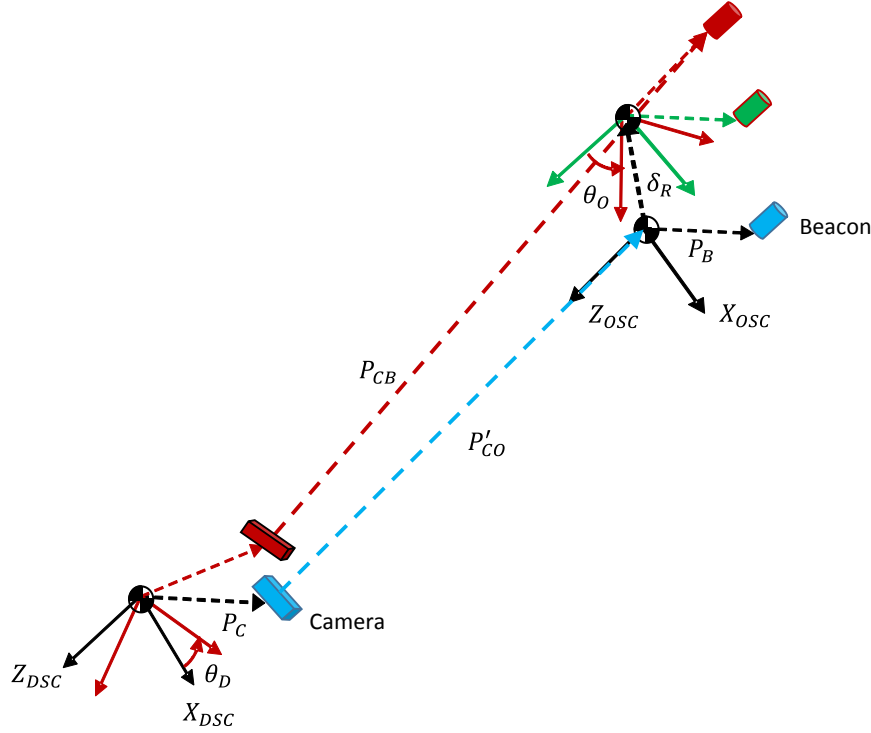
Figure 3. Alignment Camera line-of-sight as function of Attitude and Translation.

An alignment camera (e.g. similar to the Advanced Video Guidance Sensor (AVGS)[11,12]) mounted on the Detector S/C can be also be used to measure the relative S/C alignment by tracking laser beacons or retro reflectors mounted on the Optics S/C. The measurement model for this camera-based sensor can be derived as follows. From inspection of Fig. 3 it is deduced that the location of a tracked laser beacon, on Optics S/C, relative to the alignment camera image plane center, $\vec{P}_{CB}$, is expressed in terms of the spacecraft relative translational $\vec{\delta}_R$, and absolute rotational, $\vec{\theta}_D$, $\vec{\theta}_O$ DoF as,

$$\vec{P}_{CB} = \left[\vec{P}_C + \vec{P}_{CO}^{'} + \vec{\delta}_R + R(\vec{\theta}_O)\vec{P}_B \right] - R(\vec{\theta}_D)\vec{P}_C . \tag{6}$$

Then, the laser beacon spot centroid on the camera image can be expressed in terms of angles, θ_x, θ_y.

$$[\theta_x, \theta_y] = atan\left(\frac{\hat{P}_{CB}(2)}{\hat{P}_{CB}(3)}\right), atan\left(\frac{\hat{P}_{CB}(1)}{\hat{P}_{CB}(3)}\right) . \tag{7}$$

III.   VT Dynamics and Controls Framework for GN&C System Design

A complete framework for the VT GN&C system design for PFF combines the optical sensor measurement models, given in Sec. II with dynamics and inertial sensor models provided in this section. The relative flight dynamics of two spacecraft in formation has been previously studied by numerous authors with applications to formation flying technology development [5]. These generally fit into two categories: 1) formation dynamics in a close orbit to a single gravitational body (e.g. low Earth orbit) and 2) deep space applications. In this paper, we use Luquette's formulation[6-9] of the relevant dynamics in an inertial reference as a basis for the GN&C design and analysis. The dynamic equations of motion in a simplified form for the Optics S/C with respect to the Detector S/C,

given herein, are a summary of the results from Calhoun[5] with modifications to Luquette's formulation to include additional gravitational bodies and to develop the equation parameters in terms of the Detector S/C reference for ease of implementation in autonomous Leader/Follower formation architecture. The dynamics model also includes three-axis attitude dynamics for both Optics S/C and Detector S/C.

A. VT Dynamics Model Formulation

The translational dynamics of relative motion can be expressed in term of the relative position of Detector S/C with respect to the Optics S/C (Note that $[I]$ represents the 3x3 identity matrix.).[5]

$$\ddot{\bar{x}} = -\sum_{i=1}^{n} \frac{\mu_i}{\|\bar{r}_{iF}\|^3}\left([I] - 3\hat{r}_{iF}\hat{r}_{iF}^{T}\right)\bar{x} + \Delta\bar{f}_{solar} + \Delta\bar{f}_{pert} + \bar{u}_{thrust,F} - \bar{u}_{thrust,L} \quad (8)$$

Since these equations of motion for dual-spacecraft relative dynamics are developed in a general linear parametric form, they are suitable for design and evaluation of VT GN&C systems in a variety of applications. This model can be applied to control and estimation during all phases of a typical dual-spacecraft formation flying mission, including formation reorientation, initial formation alignment acquisition, and precision alignment operations. Formation flying for the virtual telescope in a Leader/Follower architecture is facilitated by using this form of the relative dynamics, since 1) the equations are expressed in an inertial reference frame and 2) the gravitational body ephemeris data are expressed relative to the follower reference.

A linear time-invariant form of Eq. 8, is formulated by expressing the relative position state, $\bar{x}$, in terms of a perturbed range state, $\bar{\delta}_R$, and a nominal reference range, $\bar{R}^{ref}$, between the two spacecraft for the virtual telescope configuration.

$$\bar{x} = \bar{R}^{ref} + \bar{\delta}_R \quad (9)$$

$$\ddot{\bar{\delta}}_R = \Gamma_{GG}\,\bar{\delta}_R + \Gamma_{GG}\bar{R}^{ref} + \bar{u}_R \quad , \quad (10)$$

where, Γ_{GG}, is a gravity gradient parameter matrix, expressed in terms of fixed parameters referenced to the follower.

$$\Gamma_{GG} = -\sum_{i=1}^{n} \frac{\mu_i}{\left\|\bar{r}_{iF}^{ref}\right\|^3}\left([I] - 3\hat{r}_{iF}^{ref}\left[\hat{r}_{iF}^{ref}\right]^T\right) \quad (11)$$

Equations (10) and (11) then form a linear time-invariant dynamics model for representation of the relative dynamics of dual-spacecraft formation when considering small displacements from a fixed relative reference trajectory. Approximations used to arrive at this final linear form are particularly applicable to a tight inertial-configured dual-spacecraft formation (e.g. a virtual telescope) in a deep space environment. In these applications, Γ_{GG} is nearly constant for short time periods associated with scientific observations.

The complete dynamics model for the dual-spacecraft formation alignment GN&C will also include the rigid body attitude equations of motion, for both Detector and Optics S/C, as given in the general form of Eqns. (12) and (13). This results in a nine DoF state model which is coupled thru optical measurements of relative position, when considering sensor locations not coincident with respective spacecraft center of mass, as shown in Eqns. (5) and (6).

$$\dot{q} = \tfrac{1}{2}\tilde{\Omega}q \quad (12)$$

$$\dot{\bar{\omega}} = I^{-1}\left(\bar{\omega}\times I\bar{\omega}\right) + \bar{T} \quad (13)$$

Measurement models for GN&C design should also include those for rate gyros, Eq. (14), and accelerometers, Eq. (15) [5].

$$\dot{\bar{\theta}} = \bar{\omega}_F{}^m - \bar{b}_{\omega_F} + \bar{v}_{\omega_F} \,, \tag{14}$$

$$\ddot{\bar{\delta}}_F{}^m = \left([I] - r_A^x \, I_F^{-1} r_T^x \, m_F\right)\bar{u}_{F_{T_0}} + \left([I] - r_A^x \, I_F^{-1} r_T^x \, m_F\right)\overline{\delta u}_{F_T}$$

$$+ \left([I] - r_A^x \, I_F^{-1} r_E^x \, m_F\right)\bar{u}_{F_E} + \bar{b}_A + \bar{v}_A \tag{15}$$

The complete framework for the VT GN&C design includes dynamics models (Eq. 8-13), measurement models for optical sensors (Eq. 1-7), and inertial sensors (Eq. 14-15).

IV. Case Study: GN&C Design for a Heliophysics Mission

The modeling framework for GN&C design, as provided in Sec. II and III, was applied to an example problem to illustrate the performance trades inherent in dual-spacecraft PFF for VT applications. The dual-spacecraft PFF technology has many applications in various scientific investigations that require a long baseline VT, such as in high energy imaging[1-4]. One such proposed Heliophysics VT mission uses a photon sieve for high resolution solar imaging[13]. The photon sieve is a type of diffractive optics for producing narrowband focused images. Achieving high resolution diffraction-limited imaging in high energy wavelengths requires long baselines, large precision manufactured optics, and precise alignment and range control stability[13]. The GN&C requirements representative of a milli-arc-sec level photon sieve application are given in Table 1. These rather precise requirements consequently place demanding specifications on GN&C architectures and sensors, particularly on optical metrology[10] needed for precise alignment sensing. The specifications for the compliment of sensor and actuators used in this study are also provided in Table 1. These values represent the approximate levels needed to achieve the given science requirements.

Table 1, Photon Sieve VT Alignment Requirements and Component Specifications

Parameter	Requirement (3σ)	Component	Specification (3σ)
Image Smear	6 microns	Laser Centration	30 microns
Depth of Field	1 mm	Laser Ranging	0.5 cm
S/C separation	200 m	Microthruster	5 μN-sec (min Impulse)
Pointing Stability (Optics S/C)	5 milli-arc sec (Sun) 10 arc-sec (roll)	Fine Sun Sensor	30 milli arc-sec
Pointing Stability (Detector S/C)	10 arc-sec	Star Tracker	6 arc-sec (transverse) 30 arc-sec (boresight)

The GN&C system design for the VT is an example of a distributed spacecraft mission involving control of two spacecraft that function together to form what is a single scientific measurement system. Depending on the placement of sensors and actuators on each spacecraft significant coupling could be present, as shown in the measurement and dynamics models provided in Sec. II and III. This implies different possible approaches to GN&C design.

When the Detector S/C is the actively controlled element for PFF of the VT, the Optics S/C (Leader) would perform only 3-axis attitude determination and control, and the Detector S/C (Follower) would perform 3-axis attitude and 3-axis relative position control. A full-state estimator (9 DoF) that processes all measurements in a single process is used to consolidate the relative state estimation for control onboard the Detector S/C. Figure 4 shows this representative sensor and actuator placement as one possible Leader/Follower architecture. Attitude control for the Optics S/C uses reaction wheels. A set of three-axis thrusters is included for momentum unloading since magnetic torqueing is not available in the target orbit (i.e. Sun-Earth libration point) for this mission. The

Detector S/C requires thrusters for relative position control so it is natural to use thrusters also for attitude control, thus avoiding the need for another set of components in the system. The Detector S/C is then configured with a full set of thrusters for 6 DoF control.
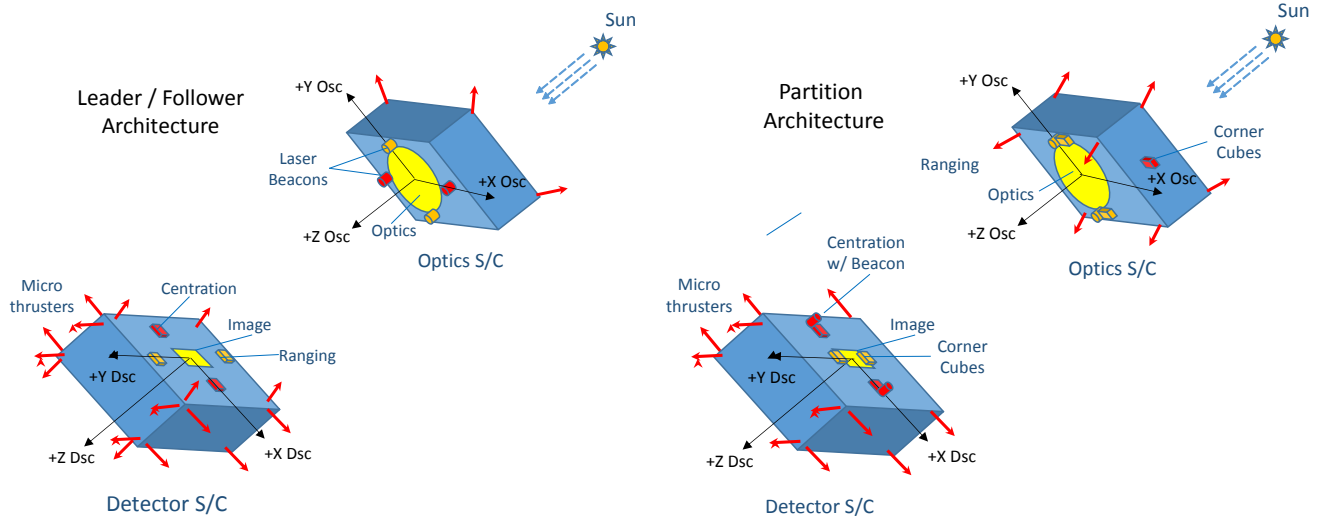

Figure 4 - Representative GN&C Architectures for the VT

This Leader/Follower architecture has two possible deficiencies. First, due to attitude coupling in the optical metrology measurements, a communication link is required to send attitude data from Optics S/C to Detector S/C for use in the full-state filter. This may suffer from possible uncertain transmission delay and timing synchronization across the inter-spacecraft communication link. Second, the thruster system for the Detector S/C is required to perform simultaneous 6-axis control. Providing a feasible thruster configuration that sufficiently decouples all axes for precision full-state control, may be difficult. The configuration shown in Fig. 4 includes a set of 24 thrusters in a 6-axis decoupled configuration. An alternate partitioned architecture design that could address these concerns is also shown in Fig. 4. In this case, the control and estimation is partitioned among the two spacecraft and the optical sensors are located to avoid the multi-platform attitude coupling in the measurement process. The Optics S/C controls the 3-axis attitude and relative range, and the Detector S/C controls the 3-axis attitude and transverse alignment only. The decoupling of laser alignment measurements on the Detector S/C and laser ranging measurements on the Optics S/C is achieved by proper placement of respective optical elements. First, laser beacons for both centration and ranging measurements are pointed to corner cube reflectors, mounted on the opposing S/C, and the return beam is acquired at a collocated detector. The use of the corner cube removes attitude dependency in the return beam (i.e. ϕ_i terms in Eq. (5) are equal to 0). The remaining attitude dependency in Eq. (5) is eliminated by locating the corner cubes for laser alignment return (on the Optics S/C) in the x-y plane, and the corner cubes for the laser ranging return (on the Detector S/C) along the z axis.

The performance of these two alternative GN&C architectures were studied in a high-fidelity Matlab/Simulink model with the complete 9 DoF dynamics. For each case, the state estimation was implemented as an Extended Kalman Filter using a continuous form for state propagation and discrete measurement updates[14]. Measurement updates were performed sequentially to avoid numerical issues associated with computation of large matrix inverses. Separate PID controllers are used for attitude and relative position states. All measurement and actuator models
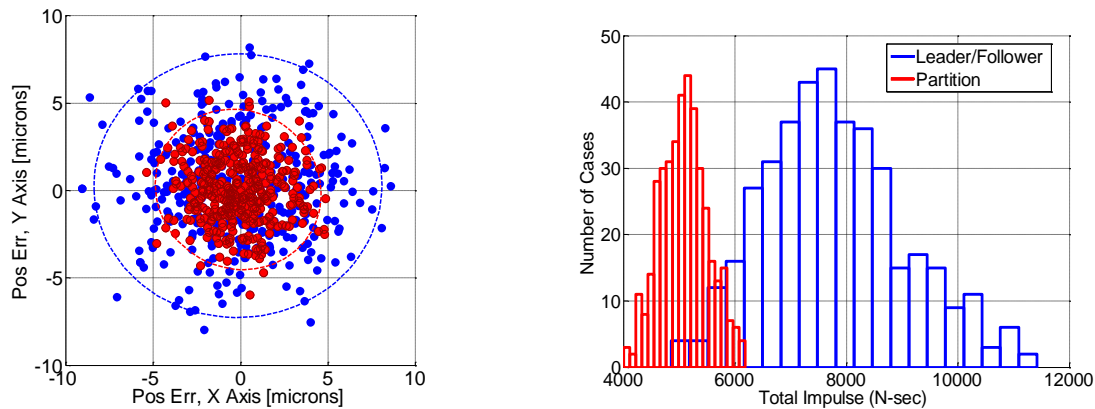

Figure 5 – Performance results of two representative GN&C architectures for the VT

include Markov processes to represent systematic errors within the control bandwidth, in addition to random noise at the levels provided in Table 1. This modelling approach facilitates assessment of the GN&C system's performance robustness in the presence of unmodeled errors.

Figure 5 shows lateral alignment error results from Monte Carlo simulations (400 cases), along with 95% confidence ellipses, for both GN&C architectures (Leader/Follower (blue), Partition (red)). Results indicate that transverse alignment errors are somewhat better for the Partition architecture. Decoupling of the laser centration measurement from the Optics S/C attitude, by the proper positioning the corner cube reflectors, results in improved transverse alignment observability in the Partition architecture. The Partition architecture performance meets the alignment requirements for the Photon Sieve application as listed in Table 1, illustrating the improvement obtained from model-based estimation over the performance of unfiltered laser sensor centration measurements. Figure 5 also shows the total impulse required for PFF over a 5 year mission for both architectures. Total impulse required to maintain alignment is significantly higher for the Leader/Follower architecture. The partitioned GN&C architecture uses about 35% less fuel because the Optics S/C, which performs range control, is half of the mass of Detector S/C. Performance comparison of these two alternative PFF architectures demonstrates the system trades that result from the measurement/state coupling and control actuator partitioning inherent in the dual S/C PFF GN&C system presented in this paper.

Conclusions

A general framework for dual-spacecraft PFF GN&C architecture design has been developed with specific application to VT missions. Development includes models for dynamics and measurement processes for systems that employ a variety of non-collocated sensors and actuators, including laser-based alignment and ranging systems, optical imaging sensors, and inertial measurement units (IMU), as well as microthrusters. A GN&C performance assessment is given for a representative Heliophysics PFF imaging mission concept. Two different GN&C architectures illustrate the potential trade-offs inherent in the choice of system architecture for this control design and mission concept.

American Institute of Aeronautics and Astronautics

Acknowledgments

References

[1] G. K. Skinner, Z. Arzoumanian, W. C. Cash et al., "The milliarc-second structure imager (MASSIM): a new concept for a high angular resolution x-ray telescope," in *Space Telescopes and Instrumentation 2008: Ultraviolet to Gamma Ray*, vol. 7011of *Proceedings of SPIE*, Marseille, France, June 2008.

[2] Cash, W., Oakley, P., Turnbull, M., Glassman, T., Lo, A., Polidan, R., Kilston, S., Noecker, C., "The New Worlds Observer: scientific and technical advantages of external occulters", SPIE, 7010, 1Q, 2008.

[3] Starin, S., "Formation Flying Mission Concept for Observing Solar Eruptive Events," *International Conference on Spacecraft Formation Flying Missions and Technologies,* May 2011.

[4] Dennis, B. R., Skinner, G. K., Li, M. J., Shih, A. Y. "Very High-Resolution Solar X-Ray Imaging Using Diffractive Optics," Solar Physics, Vol. 279, 2012, 573-588

[5] Calhoun, P., Shah, N., "Covariance Analysis of Astrometric Alignment Estimation Architectures for Precision Dual Spacecraft Formation Flying." *AIAA Guidance, Navigation, and Control Conference*.

[6] Luquette, R. J. and Sanner, R.M., "Spacecraft Formation Control: Managing Line-of-Sight Drift Based on the Dynamics of Relative Motion," *Formation Flying Symposium*, April 2008.

[7] Luquette, R. J. and Sanner, R. M., "Linear State-Space Representation of the Dynamics of Relative Motion, Based on Restricted Three Body Dynamics," *AIAA Guidance and Control Conference*, August 2004, Paper No. AIAA-2004-4783

[8] Luquette, R. J. and Leitner, J. and Gendreau, K. C. and Sanner, R. M., "Formation Control for the MAXIM Mission," *2nd International Symposium on Formation Flying Mission & Technologies*, September 2004.

[9] Luquette, R. J., "Nonlinear Control Design Techniques for Precision Formation Flying at Lagrange Points," Ph.D. Dissertation, Department of Aerospace Engineering, University of Maryland, College Park, MD, December 2006.

[10] Novo-Gradac. A., "Relative Position Sensing System for a Precision Formation Flying Space Telescope," *9th International Workshop on Satellite Constellations and Formation Flying,* Boulder, Co., June 19-21, 2017.

[11] Howard, R.T., Heaton, A. F., Pinson, R. M., Carrington, C. L., Lee, J. E., Bryan, T. C., ... & Johnson, J. E. (2008, January), „The advanced video guidance sensor: orbital express and the next generation". In M. S. El-Genk (Ed.), *AIP Conference Proceedings* (Vol. 969, No. 1, pp. 717-724). AIP.

[12] Bryan, T. C., Howard, R., Johnson, J. E., Lee, J. E., Murphy, L. and Spencer, S. H., "Next Generation Advanced Video Guidance Sensor," *2008 IEEE Aerospace Conference*, Big Sky, MT, 2008, pp. 1-8

[13] Davila, J. M. High-resolution solar imaging with a photon sieve. Proc. SPIE 8148, Solar Physics and Space Weather Instrumentation IV, 81480O (October 06, 2011

[14] Gelb, A. (ed.), *Applied Optimal Estimation*, The MIT Press, Cambridge, MA, 1974